

SECTION V

JETS, SUPERLUMINAL MOTIONS AND BLAZARS

IONIZATION AND KINEMATICS OF THE NARROW LINE REGION IN SEYFERT GALAXIES

A. S. Wilson
Astronomy Program
University of Maryland
College Park
MD 20742
U.S.A.

ABSTRACT. Direct imaging of Seyfert galaxies in emission lines and high resolution radio mapping often show their narrow line regions and linear (double or jet-like) radio sources to be aligned on the hundreds of parsecs scale. This relationship is unlikely to reflect ionization of the thermal gas by the expanding radio components or by their relativistic electrons. The most likely explanation, which is also favored by optical polarization measurements, is that ionizing photons escape preferentially along the rotation axis of the same inner (\lesssim pc scale) disk as collimates the radio jet. Such a bipolar form may be the most common morphology of the narrow line region. Differences of radio properties between Seyfert type 1's and 2's may be at least partially related to aspect effects. The north east radio lobe of NGC 1068 shows a limb-brightened, conical structure with the magnetic field running parallel to the edge of the cone. This source is modelled in terms of a radiative bow shock wave being driven into the interstellar medium of the galaxy by the radio ejecta. If the pre-shock density is as high as 400 cm^{-3} , as suggested by CO measurements, the shock velocity is found to be $\approx 75 \text{ km s}^{-1}$ and the jet velocity $\approx 4000 \text{ km s}^{-1}$, the latter being close to the emission line widths. The narrow line region in this galaxy is morphologically and kinematically associated with the jet.

1. INTRODUCTION

The optical spectra of Seyfert galaxies are characterized by intense, broad emission lines covering a wide range of ionizations and critical densities. As is well known, the emission line gas is conventionally divided into two distinct components, a compact "broad line region" (BLR) with fast moving ($\sim 10^4 \text{ km s}^{-1}$), high density clouds, and a more extended "narrow line region" (NLR) where the velocities ($\lesssim 10^3 \text{ km s}^{-1}$) and densities are lower. A combination of observational and theoretical arguments has led to a picture in which the BLR is composed of clouds with densities $N_e \approx 10^9\text{-}10^{11} \text{ cm}^{-3}$ at a distance $\approx 10^{18} \text{ cm}$ from the nucleus, while the NLR is characterized by densities $N_e \approx 10^2\text{-}10^7 \text{ cm}^{-3}$ some $10^{19}\text{-}10^{21} \text{ cm}$ from the center. In both regions, the line

emitting clouds occupy a small fraction of the overall volume. It is generally agreed that the gas in both regions is photoionized by a continuum source, the spectrum of which resembles a power law. Such photoionization models have achieved broad success (with some exceptions) in accounting for the line ratios - see e.g. the reviews by Davidson and Netzer (1979) and Ferland and Shields (1985).

The angular extent of the BLR is expected to be $\lesssim 0''.01$ in the nearest Seyfert galaxies and it will remain unresolved for the foreseeable future. Its geometrical shape is unknown and virtually all imaginable configurations (spherical, disk-shaped, conical ...) and kinematic behaviors (outflow, inflow, rotation ...) have been considered (see reviews by Osterbrock 1985 and by Mathews and Capriotti 1985). On the other hand, the NLR is sufficiently extended in nearby objects to permit direct resolution with ground-based radio, optical and infrared observations. Further, the preferred blue-wing asymmetry of $[OIII]\lambda 5007$ is a clear indication that the motions are predominantly radial (Heckman et al. 1981), although the sense - inflow or outflow - is still debated (see e.g. Wilson and Heckman 1985).

The present paper reviews recent high resolution observations which have greatly clarified the morphology and origin of the NLR. I shall also describe rather detailed investigations of NGC 1068 which have revealed that much of the high velocity emission line gas is associated with the radio ejecta ("jet") and also with the blast wave that these ejecta have driven into the interstellar medium of the surrounding galaxy.

2. STRUCTURE OF THE NARROW LINE REGION

2.1. Radio Continuum Observations

Our radio investigations of Seyfert galaxies with the Very Large Array (VLA) have concentrated on two samples, the first being based on Markarian's surveys and the second comprising all known Seyferts within a given distance (see Ulvestad and Wilson 1984a, b for further details and sample definition; a review is given by Wilson and Heckman 1985). Ulvestad and I have recently extended the survey of the distance limited sample at 6 and 20 cm to include all 51 Seyfert galaxies known as of mid-1985 with recession velocity below 4600 km s^{-1} (Huchra 1985), and declinations accessible to the VLA. Radio emission was detected from the nuclei of 48 of these.

As described in our papers, the radio structure of each galaxy has been classified into one of six morphological categories, denoted as follows:

- L = Linear (double, triple or jet-like).
- D = Diffuse ("blob-like" radio morphology).
- L+D = Both linear and diffuse sources present.
- A = Ambiguous.
- S = Slightly resolved.
- U = Unresolved.

The breakdown of each sample into these structural classes is illustrated in Table I. The numbers for the distance limited sample are

TABLE I
Radio Structural Classes of Seyfert Galaxies

Radio Structure Class	Flux Limited Sample of Markarian Seyferts	Distance Limited Sample
L	8/29 (28%)	14/48 (29%)
D	1/29 (3%)	2/48 (4%)
L+D	0/29 (0%)	2/48 (4%)
A	2/29 (7%)	3/48 (6%)
S	12/29 (41%)	16/48 (33%)
U	6/29 (21%)	11/48 (23%)

preliminary and may change slightly during our continuing analysis. Despite the omission of galaxies without strong ultraviolet excess (especially Seyfert 2's) from the Markarian sample, and possible incompleteness in the distance limited sample, the breakdown of radio structures is quite similar in the two groups. The nuclear radio sources in $\approx 60\%$ of each sample are too compact to be well mapped (classes S and U) even with the $0''.4$ resolution of the VLA in "A" configuration at 6 cm. Most of these sources have steep radio spectra and presumably represent mainly a simple continuation of the well resolved classes to smaller linear scales. The great majority of the well resolved sources fall in the L category, with only a minority being classified as D. In a couple of cases both a compact L and a more extended D component are seen; these are referred to as L+D. It is quite likely that other galaxies contain similarly composite structures. Extended D class emission may be missed in L dominated sources if it is too faint, whereas L class structures may be present in D class objects and too compact to be resolved. Our classification is intended to refer to the dominant structural type on several arc second and sub arc second scales.

The D class objects appear to be Seyfert galaxies with circumnuclear starbursts (Wilson 1986). Emission lines from the HII regions and mid-infrared emission features of dust are seen in off-nuclear spectra. Since I am primarily concerned in this article with the Seyfert activity itself, I shall not consider these composite objects further.

2.2 Relation Between Relativistic and Thermal Gases

In contrast to the "diffuse" radio sources, the "linear" objects are probably fuelled by the active nucleus in a low power version of the radio galaxy phenomenon. Fig. 1 shows the morphological relationship between the nonthermal radio continuum and the high excitation narrow line region in 6 Seyfert galaxies with "linear" radio sources. The

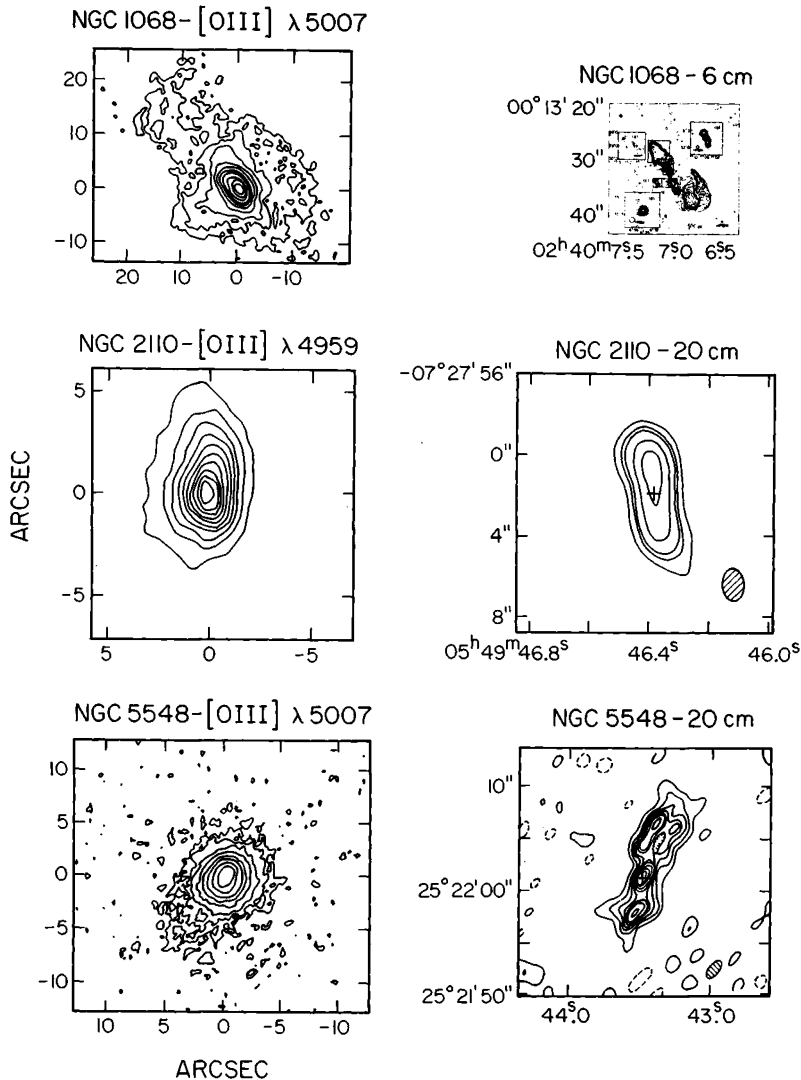


Figure 1. The relation between the high excitation narrow line region (left hand diagram) and the nonthermal radio continuum emission (right hand diagram) in 6 Seyfert galaxies with "linear" radio sources. Each pair of diagrams of any galaxy is reproduced to the same scale. NGC 1068: [OIII] λ 5007 image from Balick and Heckman (1985), 6 cm image from Wilson and Ulvestad (1983). NGC 2110: [OIII] λ 4959 image from Wilson, Baldwin and Ulvestad (1985), 20 cm image from Ulvestad and Wilson (1983). NGC 5548: [OIII] λ 5007 image from T. M. Heckman and B. Balick (private communication), 20 cm map from Wilson and Ulvestad (1982). NGC 5643: H α and 6 cm images from Morris et al. (1985). NGC 5929: [OIII] λ 5007 image from Whittle et al. (1986), 6 cm image from Ulvestad and Wilson (1984b). Mark 34: [OIII] λ 5007 image from C. A. Haniff and M. J. Ward (private communication), 20 cm image from Ulvestad and Wilson (1984a).

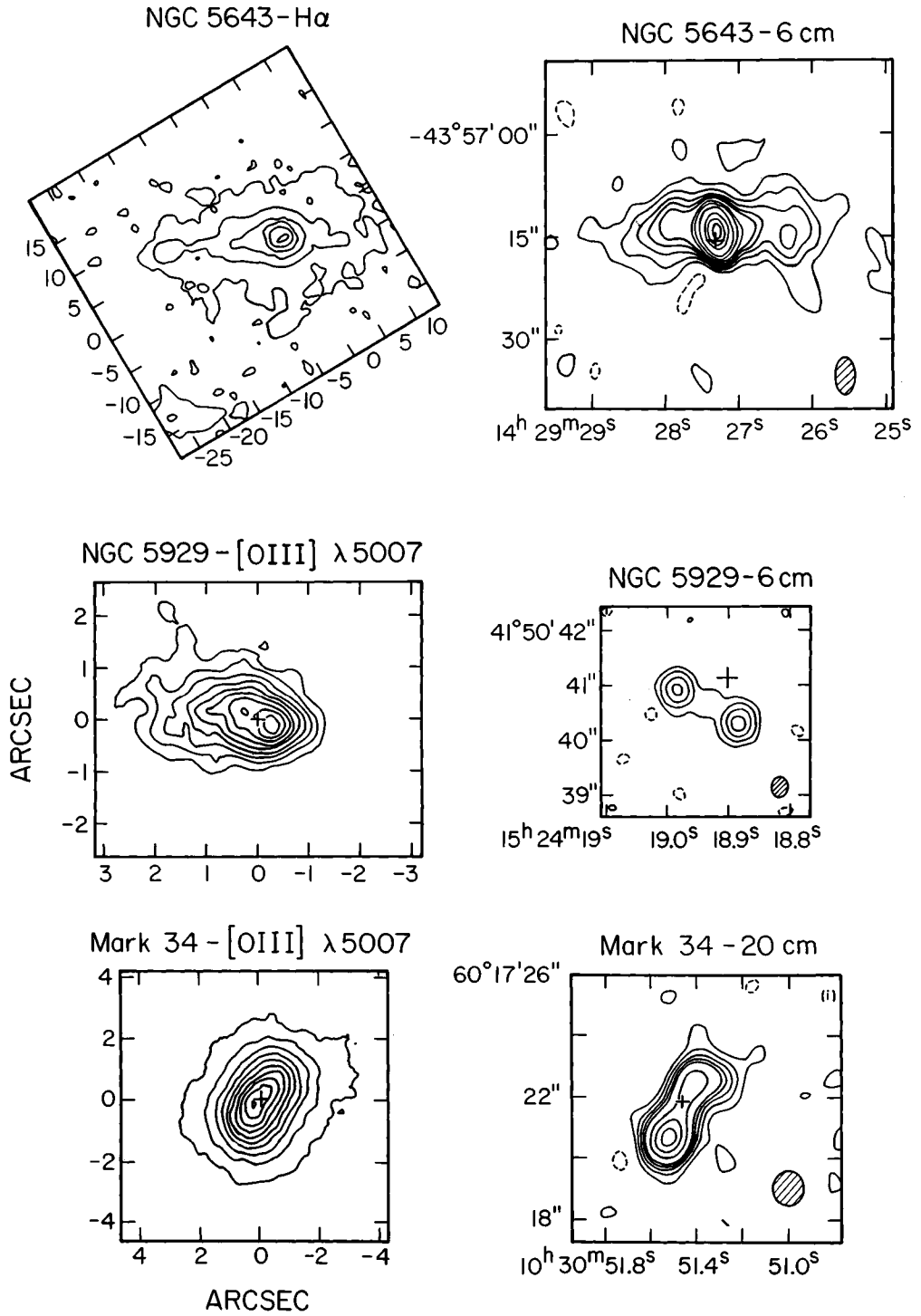


Figure 1 (continued).

following points may be noted from this figure:

- i) There is a very strong tendency for the major axes of the radio continuum and optical line distributions to be aligned. Other linear radio sources, like Mark 78 (Adams 1973; Ulvestad, Wilson and Sramek 1981) and NGC 4151 (Ulrich 1973; Booler, Pedlar and Davies 1982) are known to show a similar alignment with their narrow line cloud complexes.
- ii) A detailed correspondence between radio lobes and ionized gas is not seen in most cases. Even though they share the same major axis, the optical line emission is often more centrally concentrated than the radio continuum, as also noted by Whittle (1986).

There are two quite separate questions raised by these observations:

What is the kinematic relation between the radio ejecta and the emission line gas? and
 Why does the gas seem to be preferentially ionized along the same axis as the radio source?

A kinematic connection between the two components is suggested by the correlation between total radio power and $[OIII]\lambda 5007$ width in Seyfert galaxies (e.g. Whittle 1985). The following suggestions have been made as to the origin of this correlation. a) The narrow line region represents ambient interstellar gas which has been entrained inside the radio jet which is inferred to fuel the radio lobes (Wilson 1982). This picture is consistent with point (ii) above, that the high velocity optical line emission is concentrated between the radio lobes and the optical nucleus. Recently, the relation between the narrow line gas and the radio jet in NGC 1068 has been found to be very close (Cecil, Tully and Bland 1986). Obviously much theoretical work needs to be done concerning expected line profiles and cloud formation, dynamics and survival before such a model can be considered physically viable (e.g. Nittman, Falle and Gaskell 1982; Allen 1984). b) Pedlar, Dyson and Unger (1985) have proposed that the ambient gas is shocked, accelerated and compressed at the interface between the rapidly expanding radio lobes and the interstellar gas. While such a gaseous component must exist, point (ii) above suggests that most of the narrow line region gas is not accelerated at the boundary of the main observed radio lobes. c) the correlation may be indirect, resulting from mutual dependences of the radio power and line width on a third parameter. Obvious candidates for this parameter include the galaxy (bulge?) mass and luminosity (e.g. Hummel 1981; Meurs and Wilson 1984; Pedlar, Dyson and Unger 1985).

The origin of the apparently preferred ionization of the gas along the axis of the radio source has been less discussed. Possibilities relevant to this question include ionization and heating of the gas 1) in shock waves driven by the radio ejecta, 2) by relativistic particles, the presence of which is unambiguously indicated by the nonthermal radio emission, and 3) by the canonical, central ultraviolet source

(conventional photoionization model). In this last case, the ionizing photons would have to escape preferentially along and around the radio axis.

The spatial displacement between the radio lobes and most of the optical line emission does not favor either 1) or 2). There may be additional difficulties for 1) in the off-nuclear emission line ratios (which are often similar to those expected for power law photoionized gas - see e.g. Balick and Heckman 1979) and in energetic considerations. The kinetic power available from the outwardly moving radio components is unknown; it is conventionally related to the observed radio power through an "efficiency" factor. Because the luminosity in (narrow) emission lines is typically 10^2 - 10^3 times the radio luminosity, the kinetic power must be at least this factor larger than the radio luminosity if 1) is to be viable even from an energetic point of view. Such schemes are probably more relevant to steep spectrum cores of radio galaxies (e.g. van Breugel, Miley and Heckman 1984) or to active galactic nuclei with very weak, or absent, central ionizing sources (e.g. Ford et al. 1985) than to Seyfert galaxies.

The effect of the relativistic particles in heating and ionizing the thermal gas has been considered most recently by Ferland and Mushotzky (1984; see also Ulvestad 1981). Under certain simplifying assumptions, they calculated the ratio of the rates of relativistic electron (ξ) to photoelectric (Q) heat input, and the ratio of the ionization rate by relativistic particles (Γ^*) to the ionization rate by conventional photoionization (Γ). Their equations (9) and (10) may be recast:

$$\frac{\xi}{Q} = \frac{0.04\beta P_{\text{rel}}}{P_{\text{th}}} \quad (1)$$

$$\text{and} \quad \frac{\Gamma^*}{\Gamma} = \frac{0.083}{U} \times \frac{1.4 \times 10^{-7} P_{\text{rel}}}{P_{\text{th}}} \quad (2)$$

where β is the ratio of total heating by the cosmic rays to Coulomb heating (β takes into account collective effects - see e.g. Scott et al. 1980), P_{rel} is the relativistic electron pressure, P_{th} is the thermal pressure, and U is the ionization parameter ($U = Q(H)/4\pi N_e r^2 c$, with N_e the thermal electron density and r the separation between the ionizing source and the cloud in question). Since $P_{\text{rel}} \approx P_{\text{th}}$ in the narrow line region (e.g. de Bruyn and Wilson 1978; Pedlar, Dyson and Unger 1985) and $U \approx 10^{-2}$ in narrow line region models (e.g. Ferland 1981), it appears that the relativistic electrons are an insignificant source of ionization (as also concluded by Ulvestad 1981), but a possibly significant source of heating. Some effects of the cosmic rays on the detailed emission line ratios were calculated by Ferland and Mushotzky (1984). Many uncertainties remain, such as the effect of the magnetic field in impeding the progress of the cosmic rays into the clouds, the magnitude of collective effects, and the densities of relativistic and

subrelativistic protons.

Possibility 3) - anisotropic escape of ionizing photons along and around the radio ejection direction - is the most promising. An inner disk is needed to collimate the radio ejecta, and Osterbrock (1983) has suggested that this disk, perhaps the BLR, is optically thick to rays in the equatorial plane, so that ionizing radiation can escape only a cone around the rotation axis. The idea has a number of strong points:

α) The emission line spectrum may be accounted for in terms of the standard photoionization models (e.g. Ferland and Shields 1985) with relatively little modification.

β) In NGC 1068 and NGC 2110, the ultraviolet, nonstellar, ionizing continuum, as estimated by extrapolation of the optical or ultraviolet observations and the assumption of isotropic escape, fails to provide enough photons to account for the hydrogen line emission (Neugebauer et al. 1980; Wilson, Baldwin and Ulvestad 1985). However, if the radiation is supposed to escape preferentially along the disk's rotation axis, the luminosity of the ionizing continuum, as judged from Earth, may be much lower than actually "seen" by the forbidden line clouds (Wilson and Ulvestad 1983; Antonucci and Miller 1985). In NGC 2110, the [OIII] emission is elongated along the radio jet, but the gaseous velocity field seems kinematically undisturbed by it. In this case, it appears that relatively quiescent disk gas is being lit up by the "beamed" ionizing radiation.

γ) Unger et al. (1986) have recently obtained long slit optical spectra of a number of Seyferts with linear radio sources. They find very extended, narrow, high excitation, optical emission lines, extending much further along the radio axis than perpendicular to it. Since this gas lies well beyond the radio components, there seems no question of it being ionized by their kinetic energy or by relativistic particles. Unger et al. (1986) conclude that this "very narrow line region" is ionized by the central source, with the photons escaping preferentially along or near to the radio axis. In similar vein, Baldwin, Wilson and Whittle (1986) find that the high excitation gas in NGC 1068 is elongated along the radio axis on arc sec to arc min scales.

δ) Antonucci and Miller (1985) have shown that the optical polarized flux spectrum of NGC 1068 closely resembles the flux spectrum of a Seyfert type 1, with broad Balmer lines of $FWZI \approx 7500 \text{ km s}^{-1}$. According to their interpretation, a torus of obscuring material surrounds the BLR and compact continuum source, preventing direct observation from Earth. A small fraction of the broad line and continuum radiation is scattered into our line of sight by a warm electron gas at high latitude, which also polarizes the radiation. The axis of the torus required by the polarization observations is close to the direction of the radio jet. Further, Antonucci (1983) found that the optical polarization vector tends to align with the radio axis in type 1 Seyferts and be perpendicular to it in type 2's, so the presence of such toruses may be a general feature of Seyfert galaxies.

The conclusion of this work is that radio emitting plasma, ionizing photons and, in some cases, broad line region photons all escape

preferentially along the rotation axis of an inner disk. If our line of sight is close to the plane of such an obscuring disk or torus, and the broad lines and optical continuum radiation originate from close to its center, these radiations may only be visible via scattering by electrons above or below the disk plane (Antonucci and Miller 1985). If some type 2 Seyfert galaxies have broad line regions obscured in this way (e.g. Lawrence and Elvis 1982), the apparently larger sizes of the radio sources in type 2's than in type 1's (Ulvestad and Wilson 1984a, b) may be partially an aspect angle effect, since the radio axes of the former would tend to lie perpendicular to the line of sight. The idea may also be relevant to the higher ratio of radio to nonstellar optical continuum light in the type 2's than the type 1's, since the optical continuum observed in the type 2's would be depressed by disk obscuration.

3. RECENT WORK ON NGC 1068

NGC 1068 is a nearby Seyfert galaxy with a bright, linear radio source of large angular size ($\sim 13''$) and unusually bright, broad and spatially extended forbidden lines. The galaxy allows a clearer view of the details of the circumnuclear environment than any other Seyfert and is a rewarding object for study. Here I shall describe some recent developments in our understanding of its radio and optical properties, along with a discussion of the implications.

3.1 Radio Continuum Mapping

Fig. 2 is a 4.9 GHz map of the central regions of NGC 1068, showing the nuclear source and the oppositely directed, jet-like features feeding two radio lobes (see Pedlar et al. 1983, Wilson and Ulvestad 1983, and Ulvestad, Neff and Wilson 1986 for recent discussions). Here I should like to concentrate on the northeast radio lobe, which has an intriguing morphology. It is roughly triangular in projected shape, has very sharp edges on the E, N and NW sides, and is strongly limb-brightened. Fig. 3, which is an unpublished 15 GHz VLA map of this lobe with resolution $0''.13$, shows the limb-brightening very clearly, and also shows that the brightening is greatest at the north east ("leading") edge. The three dimensional structure of this lobe apparently approximates to that of a cone, with axis in P.A. 33° , apex $5''.6$ from the nucleus and with enhanced radio emissivity on or near its edges.

We have also mapped the linear polarization of NGC 1068 at 15 GHz. Fig. 4 shows the distribution of polarized flux vectors over the lobe at $0''.4$ resolution. Faraday rotation should be small at this frequency, so the vectors will be perpendicular to the local magnetic field direction projected onto the plane of the sky. The remarkable result is that the magnetic field runs parallel to the lobe edge in all the limb-brightened regions.

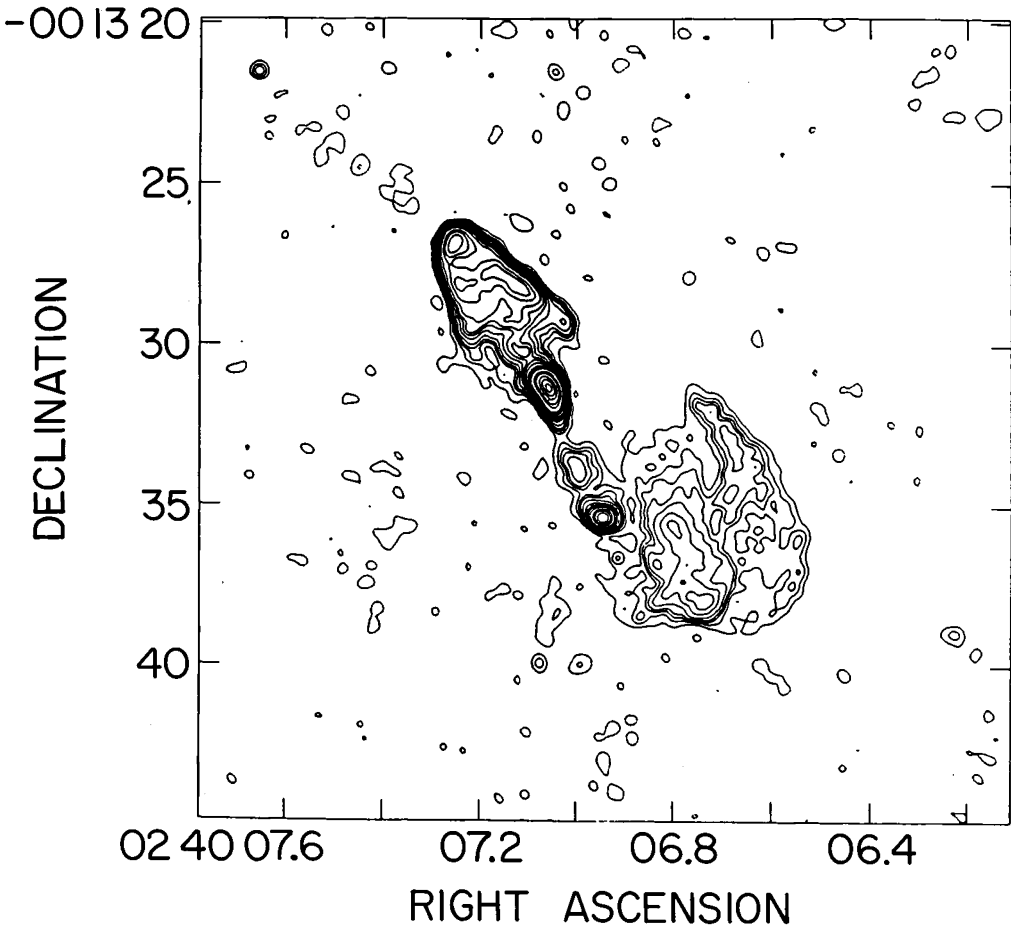


Figure 2. 4.9 GHz map of NGC 1068 with $0''.4$ resolution. See Wilson and Ulvestad (1983) for further details.

3.2 Radiative Shock Wave Model of the North East Radio Lobe

In this Section, I summarize a model of the north east radio lobe of NGC 1068 based on our suggestion (Wilson and Ulvestad 1983) that it represents a bow shock wave driven into the interstellar medium of the galaxy by the collimated nuclear ejecta ("jet" or "plasmoids", cf. Fig. 5). The arguments in favor of this point of view are:

- a) the conical, limb-brightened radio morphology,
- b) the sharp leading edge,
- c) the very large change in synchrotron emissivity across the boundary of the lobe, and
- d) the fact that the magnetic field, as deduced from the 15 GHz polarization, runs parallel to the sides of the lobe.

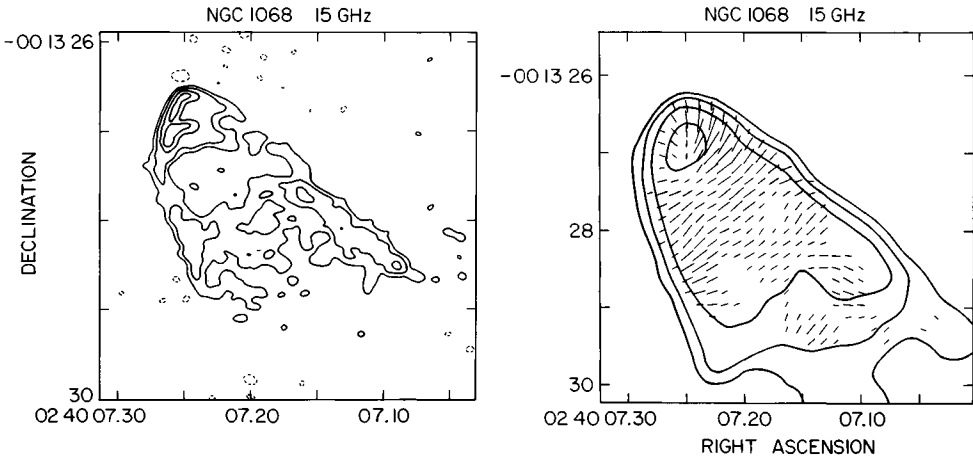


Figure 3 (left). 15 GHz map of the north east radio lobe of NGC 1068 with $0''.13$ resolution. Contours are plotted at -0.5% (dotted), 0.5% , 1% , 2% , and 3% of $49 \text{ mJy (beam area)}^{-1}$. Note the strong limb brightening at the surface of the conical lobe (data obtained in collaboration with J. S. Ulvestad).

Figure 4 (right). Electric vectors of linear polarization at 15 GHz over the north east lobe of NGC 1068 with $0''.4$ resolution. A vector length equivalent to $1''$ corresponds to 3.13 mJy of polarized flux. The contours are of total intensity at the same frequency and resolution and are plotted at 0.3% , 1% , 3% , and 10% of $83.0 \text{ mJy (beam area)}^{-1}$ (data obtained in collaboration with J. S. Ulvestad).

While these arguments strongly favor a shock wave interpretation, they do not clearly distinguish between the external ("bow") shock in the interstellar medium and the internal ("reverse") shock in the ejecta themselves. In the latter picture, the enhanced radio emission would result from compression of the magnetic fields and cosmic rays within the ejecta as they are decelerated inside the contact discontinuity with the external medium. Here my aim is to summarize the external shock model, and demonstrate that the radio emission can be fully accounted for in terms of compression of ambient interstellar cosmic rays and magnetic fields in the disk of the galaxy. The details will be published elsewhere.

3.2.1. The Radiative Shock. First I show that the shock is almost certainly radiative. The criterion separating radiative and nonradiative shocks can be simply expressed in terms of the cooling column density $N_{\text{cool}} = n_0 V_s t_{\text{cool}}$, where n_0 is the preshock particle density (the subscript 0 will always refer to preshock parameters), V_s is the shock velocity and t_{cool} is the cooling time behind the shock front. A radiative shock is one in which the actual column of the

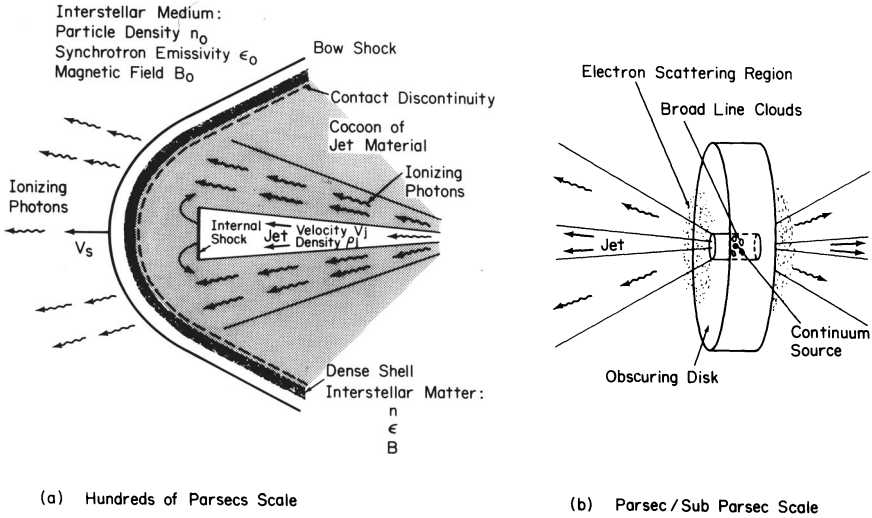


Figure 5. Schematic diagram illustrating various features of NGC 1068 (and possibly of Seyfert galaxies in general) discussed in this paper. (a) On the hundreds of parsecs scale, the jet impacts the interstellar medium of the galaxy, leading to compression in a radiative bow shock. In reality, the radio ejecta may resemble a series of individual "plasmoids" or "bubbles" more than a steady, continuous jet. Table II provides numerical estimates of some parameters. Photons escape from the nucleus preferentially along the jet axis, and ionize gas within a bi-conical or cigar shaped region, which includes both the "jet" and the dense shell of interstellar gas. The relative magnitude of the angles of the photon and jet cones is unknown. (b) Following Antonucci and Miller (1985). A thick torus hides the central broad line region and continuum source from direct view, but their radiations are partially scattered (and hence polarized) into our line of sight by an optically thin electron gas.

shocked gas $N_{tot} = n_0 d$ (where d [d_{pc} in parsecs] is the distance travelled by the shock) is greater than N_{cool} . Writing V_{s7} for the shock velocity in units of 100 km s^{-1} , and assuming that $10 > V_{s7} > 0.6$, the cooling column to 10^4 K is given approximately by (McKee and Hollenbach 1979):

$$N_{cool}(T > 10^4 \text{ K}) \approx 2 \times 10^{17} V_{s7}^{4.2} \text{ cm}^{-2} \tag{3}$$

independent of the particle density. The condition that the shock be radiative then becomes

$$V_{s7} < [15 d_{pc} n_0]^{1/4.2} \tag{4}$$

If the shock wave is envisaged to have travelled the distance between

the nucleus and its present position, we have $d \approx 5'' = 360 \text{ pc}$ ($H_0 = 75 \text{ km s}^{-1} \text{ Mpc}^{-1}$). The shock wave appears, at least in projection, to be ploughing into the inner part of the dense, molecular ring inferred by Scoville, Young and Lucy (1983) from CO observations. These authors estimated that the average density in the ring is $n(\text{H}_2) \approx 200 \text{ cm}^{-3}$. While higher resolution CO observations with the Nobeyama telescope do not confirm the ring morphology (H. Liszt, private communication), the mean density should not be too much in error. With these estimates of n_0 and d_{pc} , equation (4) gives $V_{\text{S}7} \lesssim 32$. Even if n_0 is considerably below the above estimate, the shock is expected to be radiative for all values of the shock velocity for which the above used approximation to the cooling curve is valid.

3.2.2. The Compression in the Cooling Zone. Immediately behind the shock, the gas is heated to a high temperature T_{S} . As it cools, the temperature drops and the density rises until either the temperature stabilizes at a sufficiently high value that magnetic pressure is unimportant, or magnetic pressure provides the support. An approximate solution for the relation between n and T in the cooling region is equation (2.37) of Hollenbach and McKee (1979). The cosmic rays and magnetic field are compressed along with the thermal gas, and the synchrotron emissivity is enormously enhanced. The situation is analogous to van der Laan's (1962) model for the radio emission of an old supernova remnant.

In order to apply the model, a number of parameters must first be obtained from the observations. The pre-shock synchrotron emissivity at 5 GHz ($\epsilon_{0,5}$) is derived under the assumption that the north east radio lobe of NGC 1068 is ploughing into the synchrotron radio emitting disk, which has been mapped recently by Wynn-Williams, Becklin and Scoville (1985). This assumption does not require the lobe to be ejected precisely in the plane of the disk. The tip of the lobe projects only $6'' = 430 \text{ pc}$ from the nucleus, so much or all of it must still be immersed in the disk, whatever the angle between the ejection axis and the disk plane. $\epsilon_{0,5}$ is obtained from the radio brightness just ahead of the lobe in the map of Wynn-Williams, Becklin and Scoville (1985). The pre-shock magnetic field strength (B_0) may then be derived from the usual equipartition assumption. The model has been developed for two values of the pre-shock thermal density (n_0), the first being the average density in the molecular ring (Scoville, Young and Lucy 1983) and the second a factor of ten lower. Lastly, the post-shock synchrotron emissivity at 5 GHz (ϵ_5) may be obtained from our high resolution map of the lobe at 15 GHz (Fig. 3) and the radio spectral index. The numerical values obtained are given in the top four columns of table II.

The enhancement in synchrotron emissivity across the shock ($\epsilon_5/\epsilon_{0,5}$) is thus a known parameter. It may be used to find the compression ($\chi = n/n_0$, where n is the thermal density in the dense cooled zone), since the magnetic field is assumed to be frozen to the thermal gas and the cosmic rays are tied to the magnetic field (see e.g. van der Laan 1962). From the compression, the magnetic field in the cooled zone (B) and the shock velocity (V_{S}) are obtained, the latter

under the assumption that the final temperature is 10^4K (Table II). The cooled postshock gas turns out to be magnetically supported if $n_o \lesssim 300 - 400 \text{ cm}^{-3}$.

TABLE II
Parameters of the north east radio lobe and jet of
NGC 1068 derived from the observations or the model.

Parameter	Tip of Lobe	Side of Lobe
$\epsilon_{o,5}(\text{WHZ}^{-1}\text{pc}^{-3})$	1.6×10^{12}	1.6×10^{12}
$B_o(\text{gauss})$	3.4×10^{-5}	3.4×10^{-5}
$n_o(\text{cm}^{-3})$	400 or 40	400 or 40
$\epsilon_5(\text{WHZ}^{-1}\text{pc}^{-3})$	4.4×10^{16}	9.3×10^{15}
$\chi = n/n_o$	21.0	13.5
$B(\text{gauss})$	5.9×10^{-4}	3.8×10^{-4}
$V_s(\text{km s}^{-1})$	76 ($n_o = 400 \text{ cm}^{-3}$) 140 ($n_o = 40 \text{ cm}^{-3}$)	57 ($n_o = 400 \text{ cm}^{-3}$) 96 ($n_o = 40 \text{ cm}^{-3}$)
$V_j(\text{km s}^{-1})$	4,000 ($n_o = 400 \text{ cm}^{-3}$) 12,000 ($n_o = 40 \text{ cm}^{-3}$)	
$\rho_j(\text{gm cm}^{-3})$	2×10^{-25} ($n_o = 400 \text{ cm}^{-3}$) 9×10^{-27} ($n_o = 40 \text{ cm}^{-3}$)	

Lastly, the equation of ram pressure balance between the radio jet and the interstellar gas, along with the assumption that the radio luminosity is fuelled by the jet with an efficiency factor of 0.01, allows the jet density (ρ_j) and velocity (V_j) to be calculated in terms of n_o and V_s (Table II).

3.3 Consequences of the Model

The model described in the last Section predicts a jet velocity of 4,000 - 12,000 km s^{-1} and a bow shock velocity of 75 - 140 km s^{-1} . The component of these velocities along the line of sight will be lower by the unknown projection factor. It is well known that the nuclear emission line gas in NGC 1068 is elongated to the north east, along the radio jet (Bertola 1966; Walker 1968; Alloin et al. 1981). A recent, high spatial resolution study of $[\text{NII}]\lambda 6584$ with an imaging Fabry-Perot system (Cecil, Tully and Bland 1986) beautifully confirms the jet-like form of the high velocity emission line gas over a scale of a few arc sec. In this region, the FWZI of the $[\text{OIII}]\lambda 5007$ line is $\approx 3000 \text{ km s}^{-1}$ (see Fig. 8 of Wilson and Heckman 1985). This excellent agreement of both the morphologies and line of sight velocities of the radio jet and optical emission line gas confirms the idea that the high velocity gas in the narrow line region is associated with the radio ejecta.

The images of Cecil, Tully and Bland (1986) also reveal the limb-brightened radio lobe in $[\text{NII}]\lambda 6584$ emission. This "wedge-shaped" feature is seen at velocities of several tens of km s^{-1} w.r.t. systemic, confirming the low bow shock velocity derived in the model. This gas represents compressed interstellar material in the post-shock cooling zone. A direct measurement of its density would be a most valuable constraint on the model.

4. CONCLUSIONS

Fig. 5 is a schematic diagram illustrating some of the conclusions of this paper. I have argued that "linear" structure is the most common form of radio morphology in Seyfert galaxies, that the narrow line region is commonly aligned with this radio source, and that the alignment appears to represent a common, preferential escape of radio-emitting plasma and ionizing photons along the rotation axis of an inner disk. The polarization results of Antonucci and Miller (1985) and the observations of the "very narrow line region" by Unger et al. (1986) strongly support this view. If these ideas are correct, the narrow line region must take a bi-conical, jet-like or cigar shaped form in most Seyfert galaxies. It will be interesting to confirm this picture with the high resolution imaging observations expected from the Hubble Space Telescope. The study of the hundreds of parsec scale properties of the Seyfert nucleus thus provides interesting clues to the smaller scale, unresolved and more important events closer to the central engine. The theoretical consequences for the broad line region and other sub-parsec scale entities deserve close scrutiny (cf. Krolik and Begelman 1986).

I have also summarized a simple model of the interaction between the ejected radio components and the surrounding interstellar medium (Fig. 5). The radio emission of the north east lobe of NGC 1068 may represent ambient disk cosmic rays and magnetic field compressed in a strongly radiative bow shock. If the preshock density is 400 cm^{-3} , as inferred from CO observations, the bow shock velocity is $\approx 75 \text{ km s}^{-1}$ and the jet velocity $\approx 4000 \text{ km s}^{-1}$. The close agreement between this jet velocity and the emission line widths, and the similarity of radio jet and optical emission line morphologies argues that the high velocity of the narrow line gas in Seyfert galaxies is related to outflow associated with their radio ejecta.

ACKNOWLEDGEMENTS

The new radio data presented in this paper have been obtained in collaboration with J. S. Ulvestad. I am grateful to the American Astronomical Society for a travel grant which allowed me to attend the conference, and to the Space Telescope Science Institute for hospitality while this paper was being written. I thank G. Cecil, R. B. Tully, J. Bland, T.M. Heckman, B. Balick, C. A. Haniff, and M. J. Ward for communication of unpublished data.

References

- Adams, T. F. 1973, Ap. J., **179**, 417.
Allen, A. J. 1984, M.N.R.A.S., **210**, 147.
Alloin, D., Lacques, P. Pelat, D., and Despiauw, R. 1981, Astr. Ap. Suppl., **43**, 231.
Antonucci, R. R. J. 1983, Nature, **303**, 158.

- Antonucci, R. R. J., and Miller, J.S. 1985, Ap. J., **297**, 621.
- Baldwin, J. A., Wilson, A. S., and Whittle, M. 1986, Ap. J., (submitted).
- Balick, B., and Heckman, T. M. 1979, A. J., **84**, 302.
- Balick, B., and Heckman, T. M. 1985, A. J., **90**, 197.
- Bertola, F. 1966, Pub. Obs. Padova, No. 134.
- Booler, R. V., Pedlar, A., and Davies, R. D. 1982, M.N.R.A.S., **199**, 229.
- Cecil, G., Tully, R. B., and Bland, J. 1986, Bull. A.A.S., **18**, 640.
- Davidson, K., and Netzer, H. 1979, Rev. Mod. Phys., **51**, 715.
- de Bruyn, A. G., and Wilson, A. S. 1978, Astr. Ap., **64**, 433.
- Ferland, G. J. 1981, Ap. J., **249**, 17.
- Ferland, G. J., and Mushotzky, R. F. 1984, Ap. J., **286**, 42.
- Ferland, G. J., and Shields, G. A. 1985, see Miller 1985, p. 157.
- Ford, H. C., Crane, P. C., Jacoby, G. C., Lawrie, D. G., and van der Hulst 1985, Ap. J., **293**, 132.
- Heckman, T. M., Miley, G. K., van Breugel, W. J. M., and Butcher, H. R. 1981, Ap. J., **247**, 403.
- Hollenbach, D. J., and McKee, C. F. 1979, Ap. J. Suppl., **41**, 555.
- Huchra, J. P. 1985, Catalog of Seyfert Galaxies, distributed privately.
- Hummel, E. 1981, Astr. Ap., **93**, 93.
- Krolik, J., and Begelman, M.C. 1986, Preprint.
- Lawrence, A., and Elvis, M. 1982, Ap. J., **253**, 410.
- Mathews, W. G., and Capriotti, E. R. 1985, see Miller 1985 p. 185.
- McKee, C. F., and Hollenbach, D. J. 1980, Ann. Rev. Astr. Ap., **18**, 219.
- Meurs, E. J. A., and Wilson, A. S. 1984, Astr. Ap., **136**, 206.
- Miller, J. S., ed., 1985, Astrophysics of Active Galaxies and Quasi-Stellar Objects, based on the 1984 Santa Cruz Astrophysics Workshop (University Science Books).
- Morris, S., Ward, M., Whittle, M., Wilson, A. S., and Taylor, K. 1985, M.N.R.A.S., **216**, 193.
- Neugebauer, G. et al. 1980, Ap. J., **238**, 502.
- Nittmann, J., Falle, S. A. E. G., and Gaskell, P. H. 1982, M.N.R.A.S., **201**, 833.
- Osterbrock, D. E. 1983, In IAU Symposium 103, Planetary Nebulae, ed. D. R. Flower p. 473 (Reidel, Dordrecht).
- Osterbrock, D. E. 1985, see Miller 1985 p. 111.
- Pedlar, A., Booler, R. V., Spencer, R. E., and Stewart, O. J. 1983, M.N.R.A.S., **202**, 647.
- Pedlar, A., Dyson, J., and Unger, S. W. 1985, M.N.R.A.S., **214**, 463.
- Scott, J. S., Holman, G. D., Ionson, J. A., and Papadopoulos, K. 1980, Ap. J., **239**, 769.
- Scoville, N. Z., Young, J. S., and Lucy, L. B. 1983, Ap. J., **270**, 443.
- Ulrich, M.-H. 1973, Ap. J., **181**, 51.
- Ulvestad, J. S. 1981, Ph. D. thesis, University of Maryland.
- Ulvestad, J. S., Wilson, A. S., and Sramek, R. A. 1981, Ap. J., **247**, 419.
- Ulvestad, J. S., and Wilson, A. S. 1983, Ap. J. (Letters), **264**, L7.
- Ulvestad, J. S., and Wilson, A. S. 1984a, Ap. J., **278**, 544.
- Ulvestad, J. S., and Wilson, A. S. 1984b, Ap. J., **285**, 439.
- Ulvestad, J. S., Neff, S. G., and Wilson, A. S. 1986, A. J. (in press).

- Unger, S. W., Pedlar, A., Axon, D. J., Harrison, B. A., Meurs, E. J. A., Ward, M. J., and Whittle, M. 1986, private communication.
- van Breugel, W. J. M., Miley, G. K., and Heckman, T. M. 1984, A. J., **89**, 5.
- van der Laan, H. 1962, M.N.R.A.S., **124**, 125.
- Walker, M. F. 1968, Ap. J., **151**, 71.
- Whittle, M. 1985, M.N.R.A.S., **213**, 33.
- Whittle, M. 1986, Colloquium at University of Maryland, April 2.
- Whittle, M., Haniff, C. A., Ward, M. J., Meurs, E. J. A., Pedlar, A., Unger, S. W., Axon, D. J., and Harrison, B. A. 1986, M.N.R.A.S. (in press).
- Wilson, A. S. 1982, In IAU Symposium 97, Extragalactic Radio Sources, p. 179 (Reidel, Dordrecht).
- Wilson, A. S. 1986, Ap. J. (Letters), submitted. See also related paper in Proceedings of Conference Star Formation in Galaxies, California Institute of Technology, in press.
- Wilson, A. S., and Ulvestad, J. S. 1982, Ap. J., **260**, 56.
- Wilson, A. S., and Ulvestad, J. S. 1983, Ap. J., **275**, 8.
- Wilson, A. S., and Heckman, T. M. 1985, see Miller 1985 p. 39.
- Wilson, A. S., Baldwin J. A., and Ulvestad, J. S. 1985, Ap. J., **291**, 627.
- Wynn-Williams, C. G., Becklin, E. E., and Scoville, N. Z. 1985, Ap. J., **297**, 607.

DISCUSSION

MACCHETTO: In your calculations you derived a jet velocity of ~ 4500 km s⁻¹. However, the Hawaii data showed velocities of only ~ 500 km s⁻¹. How do you explain this difference?

WILSON: The lines in NGC 1068 are actually much broader than the range of velocities included on the slide of the Hawaii images (Cecil, Tully, & Iand) that I showed. As can be seen from our distribution of [OIII] λ 5007 line profiles, the lines are fully 3000 km s⁻¹ broad at the continuum level (i.e. ± 1500 km s⁻¹ from the centre). This is in excellent agreement with the jet velocity I derived, when allowance is made for projection.

BOCHKAREV: What percentage of Seyferts have circumnucleus starbursts?

WILSON: A question like this needs to be phrased: "What fractions of Seyfert galaxies have a luminosity (in some waveband) powered by massive stars (or their effects - HII regions, SNR's etc.) greater than such and such a value?" And then: " Is this fraction significantly different from the fractions found in a comparison sample of otherwise similar, but not Seyfert galaxies?" I have shown that the nuclear region of only a small fraction of Seyferts are dominated by the diffuse radio structure associated with a luminous circumnuclear starburst. These galaxies always show off-nuclear, optically visible HII regions, far infrared spectra resembling those of HII regions and dust

emission features, which are also typical of HII regions. Most Seyferts in our optical long slit survey do not exhibit prominent circumnuclear HII regions. In this sense, the fraction of Seyferts with prominent starbursts is small.

HUTCHINGS: Are any of the linear radio sources one-sided (i.e. like many quasars)?

WILSON: Mostly we see two-sided sources straddling the optical continuum nucleus. In a few cases like NGC 4151, the structure is one-sided very close to the nucleus, but two-sided further out.

WILSON: This is closely related to Bochkarev's question. In a recent paper (to be submitted to Ap.J. Letters) I have shown that the Seyferts with 25-60-100 nm spectral shapes like nuclear starbursts are just those in which observations in other wavebands (radio continuum, optical line) also indicate active star formation. There are, however, many Seyferts with only high excitation circumnuclear gas (ionized by the central nonthermal source), "linear" (jet-like) radio sources and power law IRAS spectra. I do not consider the far infrared emission of these latter objects to be related to star formation, and thus I disagree with your number of 85%.

TERLEVICH: It is known that Sy 1's are less powerful radio emitters than Sy 2's. Can you please describe how this is explained in the plasmoid scenario?

WILSON: In the scenario I described, Seyfert 1's have developed, maybe thicker disks (perhaps associated with the broad line region) in their nuclei than do Seyfert 2's. In the Seyfert 1's this inner disk "soaks up" both ionizing photons and radio emitting plasma and prevents their escape into the narrow line region, which is where the radio emission is mainly seen. In the Seyfert 2's, the inner disk is much less efficient in absorbing the photons and plasma and correspondingly more escapes. Thus the difference in radio properties is initially associated with the broad line: narrow line ratios, as also indicated by the intermediate radio powers of intermediate type (1.5) Seyfert galaxies. This picture also accounts for the correlation between radio power and $[OIII]\lambda 5007$ power.